ELSEVIER

Advances in Water Resources 24 (2001) 595–605

Advances in Water Resources

www.elsevier.com/locate/advwatres

Adaptive time stepping and error control in a mass conservative numerical solution of the mixed form of Richards equation

D. Kavetski, P. Binning *, S.W. Sloan

Department of Civil, Surveying and Environmental Engineering, University of Newcastle, Newcastle, Callaghan, NSW 2308, Australia

Received 1 July 2000; received in revised form 1 November 2000

Abstract

Adaptive time stepping with embedded error control is applied to the mixed form of Richards equation. It is the first mathematically based adaptive scheme applied to this form of Richards equation. The key to the method is the approximation of the local truncation error of the scheme in terms of the pressure head, although, to enforce mass conservation, the principal time approximation is based on the moisture content. The time stepping scheme is closely related to an implicit Thomas–Gladwell approximation and is unconditionally stable and second-order accurate. Numerical trials demonstrate that the new algorithm fully automates stepsize selection and robustly constrains temporal discretisation errors given a user tolerance. The adaptive mechanism is shown to improve the performance of the non-linear solver, providing accurate initial solution estimates for the iterative process. Furthermore, the stepsize variation patterns reflect the adequacy of the spatial discretisation, here accomplished by linear finite elements. When sufficiently dense spatial grids are used, the time step varies smoothly, while excessively coarse grids induce stepsize oscillations.

Keywords: Richards equation; Adaptive time stepping; Conservation of mass

1. Introduction

Accurate, reliable and efficient simulations of moisture fluxes through porous media are desirable in hydrological and environmental studies, as well as in civil and environmental engineering. The ability to model time dependent flows in composite soil formations that may be intermittently saturated and drained is particularly important from the point of view of physical realism. This paper focuses on appropriate and controlled treatment of the time dependence of variably saturated flows, ensuring accuracy and efficiency in a simple and robust time stepping algorithm.

Richards equation is the mathematical model typically used to describe variably saturated flows [6]. It is defined by coupling a statement of flow continuity with the Darcy equation and is commonly cast into one of the following forms:

$$\frac{\partial\theta}{\partial t} - \nabla\cdot D(\theta)\nabla\theta + \frac{\partial K(\theta)}{\partial z} = 0 \quad (\text{moisture-based}, \theta\text{-form}), \tag{1}$$

$$\left[C(\psi) + \frac{\theta}{\phi}S_s\right]\frac{\partial\psi}{\partial t} - \nabla\cdot K(\psi)\nabla\psi + \frac{\partial K(\psi)}{\partial z} = 0 \quad (\text{pressure-based}, \psi\text{-form}), \tag{2}$$

$$\frac{\partial\theta}{\partial t} + \frac{\theta}{\phi}S_s\frac{\partial\psi}{\partial t} - \nabla\cdot K(\psi)\nabla\psi + \frac{\partial K(\psi)}{\partial z} = 0 \quad (\text{mixed, or coupled form}), \tag{3}$$

where ψ is the pressure head [L], $\theta(\psi)$ is the volumetric moisture content, t is time [T], z is the (positive downward) depth [L], ϕ is the porosity, S_s is the specific storativity [L^{-1}] and ∇ is the gradient operator with respect to the spatial coordinates x, y and z. The solution of Richards equation requires the specification of soil constitutive functions: the hydraulic conductivity $K(\psi)$ [L/T], the specific capacity $C(\psi) \equiv d\theta/d\psi$ [L^{-1}] and the diffusivity $D(\theta) \equiv K(\theta)/C(\theta)$ [L^2/T].

The combination of highly non-linear constitutive functions with non-trivial boundary and initial conditions precludes all but the most simplified analytic

* Corresponding author. Tel.: +61-2-4921-5735; fax: +61-2-4921-6991.

E-mail address: pbinning@mail.newcastle.edu.au (P. Binning).

0309-1708/01/$ - see front matter
PII: S0309-1708(00)00076-2

approaches to the solution of (1)–(3). Common practical approaches for the analysis of variably saturated flows are mixed and pressure-based numerical formulations, which employ low-order finite difference or finite element spatial discretisation and simple Euler time stepping [1,3,13,15]. The numerical stability of the temporal approximation is enforced by employing implicit (typically, backward Euler) time stepping, while oscillations in the finite element spatial discretisation are controlled by lumping [3,7]. Substantial research has also been dedicated to the solution of the non-linear discrete systems that arise in implicit time stepping schemes [9,10,13], and to the incorporation of the soil constitutive relationships [10].

In view of the discretisation error that invariably arises in numerical approximations, quality control of the convergence of the approximation to the true solution is of great importance. However, the reliability and efficiency of common temporal discretisations of Richards equation remain problematic, since very few schemes attempt to gauge internal errors or optimise time step selection.

Uniform stepsize schemes are clearly inadequate when the solution changes in character throughout the simulation. Indeed, the strong non-linearity of Richards equation, coupled with non-trivial boundary conditions encountered in practice, induce appreciable changes in the behaviour of the solution. As a result, uniform time stepping schemes may spend valuable computing time scrutinising regions of simple solution behaviour with time steps that are excessively small, while incurring large unknown errors when integrating fast non-linear flow regions, where the same time steps may be too large. It can be seen that uniform time integrators lack quality control and are computationally inefficient.

Variable stepsize schemes are now standard in ODE theory [14], yet most variable stepsize schemes applied to Richards equation are heuristic and lack generality and mathematical rigour. Heuristic methods (e.g. [15]) require manual optimisation and considerable insight of the user into the numerical performance of the algorithm. More importantly, most heuristic schemes vary the time step according to the performance of the iterative non-linear solver and do not provide a mathematically rigorous assessment of the potential numerical discretisation errors. Therefore, although in principle overcoming the efficiency shortcomings of uniform time stepping algorithms, heuristic schemes can produce unreliable or misleading results.

Recently, Tocci et al. [20], Miller et al. [10] and Williams and Miller [21] described the application of several existing variable-order variable-stepsize differential-algebraic equation (DAE) solvers (e.g., DASPK) to the pressure form of Richards equation. Sophisticated high-order methods provided appreciable improvements over existing low-order uniform-stepsize algorithms when a fine error tolerance is imposed. However, many black-box ODE integrators have certain limitations in the practical context of modelling variably saturated flows.

An appreciable advantage of a numerical scheme based on the mixed form of Richards equation is its inherent conservation of mass. Conversely, standard numerical approximations based on the pressure form of Richards equation develop undesirable mass balance problems [3], seriously undermining their physical basis. Although using DASPK to integrate in time the pressure form of Richards equation constrains mass balance errors, it could be argued that an inherently mass conservative scheme (based on (3)) is preferable. However, many standard ODE solvers are not readily applied to the mixed form of Richards equation because of the difficulty of handling two state vectors (moisture and pressure) [20]. Whilst differential-algebraic equation solvers, such as DASPK, can be used for the mixed form of Richards equation, this has not yet been done. The algorithm presented in this paper overcomes these difficulties and is the first mathematically based adaptive time stepping algorithm applied to the mixed form of Richards equation.

In practical applications where the computational speed of the solution is an important priority, numerical errors of the order of 0.1–1% are typically acceptable. In these cases low-order schemes are competitive with higher-order solvers, and may in fact be preferred due to their better stability and algorithmic simplicity [22]. Numerical experiments have shown, for example, that the second-order accurate Crank–Nicolson scheme outperformed the first-order accurate backward Euler scheme only when relative errors below 0.005% were required [22, p. 264]. The results of other numerical investigations (e.g., [13,20]) also suggest that low-order schemes are competitive with higher-order schemes when coarse time steps are used. Indeed, most practical codes implement simple first- or second-order approximations, rather than comparatively complex ODE or DAE solvers [3].

A potential limitation of some variable-stepsize time stepping schemes is that they encourage the use of a constant stepsize for significant time periods, and/or constrain the time step variation to a certain fixed pattern (e.g., halving or doubling the stepsize). The new algorithm presented in this paper does not have this constraint and employs subtler, smooth changes in stepsize. It will be shown later that the smoothness of the stepsize variation is useful in assessing the adequacy of the spatial approximation.

Recently, Sloan and Abbo [17] introduced a new approach for quality-controlled time approximation of elastoplastic consolidation in geomechanics. The scheme is based on a measure of local truncation error in the solution, which can be used to control temporal

discretisation errors, derive an efficient stepsize selector and obtain second-order accuracy at minimal computational cost. The algorithm is derived from the backward Euler scheme and hence is simple, yet very stable and robust.

In this paper, the principles of the adaptive scheme of Sloan and Abbo [17] are generalised to the more complex mixed form (3) of Richards equation. The use of the mixed form removes the limitations of pure moisture-based models in saturated regions and heterogeneous soils, while retaining the beneficial mass conservative properties. The chief advantage of the scheme is that it provides a simple and practical, yet mathematically rigorous approach for quality control in an inherently mass conservative model of variably saturated flows.

2. Algorithm development

2.1. Spatial approximation

The Galerkin finite element method offers a convenient way to separate the boundary-value spatial component of Richards equation from its initial-value temporal variation. Ignoring for the moment the soil/water compressibility terms, the finite element spatial discretisation of (3) leads to the following first-order ODE system:

$$\mathbf{M}\frac{\mathrm{d}\boldsymbol{\theta}}{\mathrm{d}t}+\mathbf{K}\boldsymbol{\psi}=\mathbf{F}, \tag{4}$$

where $\boldsymbol{\theta}$ and $\boldsymbol{\psi}$ are the nodal moisture and pressure values, $\mathbf{M}$ is the mass (or time) matrix, $\mathbf{K}$ is the conductivity matrix and the force vector $\mathbf{F}$ contains the gravity drainage term and other forcing data, including boundary conditions.

The finite element (and finite difference) method leads to the ODE system (4) regardless of the spatial dimensionality of the problem. Therefore, a temporal approximation scheme designed for (4) is immediately applicable to 1D, 2D or 3D cases. Naturally, as the number of spatial dimensions is increased, one is faced with more sources of error, yet, from the point of view of the time integration, it is still an ODE system of form (4), but with matrices $\mathbf{M}$, $\mathbf{K}$ and $\mathbf{F}$ of different structure. In this paper, the time integration algorithm is derived for the generic ODE system (4) and tested on a 1D problem. For one-dimensional vertical flows and linear basis functions, the elemental matrices are given by:

$$m_{i,j}^{(e)}=\int_0^{L(e)} N_iN_j\,\mathrm{d}z$$

$$\Rightarrow \mathbf{M}^{(e)}=\frac{L^{(e)}}{6}\begin{bmatrix}2&1\\1&2\end{bmatrix}\Rightarrow \mathbf{M}_L^{(e)}=\frac{L^{(e)}}{2}\begin{bmatrix}1&0\\0&1\end{bmatrix}, \tag{5}$$

$$k_{i,j}^{(e)}=\int_0^{L(e)} K\frac{\partial N_i}{\partial z}\frac{\partial N_j}{\partial z}\,\mathrm{d}z\Rightarrow \mathbf{K}^{(e)}=\frac{K^{(e)}}{L^{(e)}}\begin{bmatrix}1&-1\\-1&1\end{bmatrix}, \tag{6}$$

$$f_i^{(e)}=\int_0^{L(e)} K\frac{\partial N_i}{\partial z}\,\mathrm{d}z+\left[\left(K\frac{\partial\psi}{\partial z}-K\right)N_i\right]_0^{L(e)}$$

$$\Rightarrow \mathbf{F}^{(e)}=K^{(e)}\begin{bmatrix}1\\-1\end{bmatrix}+\begin{bmatrix}q_1\\q_2\end{bmatrix}, \tag{7}$$

where $L^{(e)}$ is the element length and $K^{(e)}$ is the element conductivity, evaluated as the arithmetic mean of the nodal values according to $K^{(e)}=1/2(K_1+K_2)$. To improve the numerical stability of the finite element approximation, the mass matrix $\mathbf{M}^{(e)}$ is lumped, as shown in (5). This enforces the maximum and monotonicity principles, removing undesirable oscillations from the numerical solution of the PDE [3]. Any other spatial discretisation method that leads to an ODE system similar to (4) can also be employed. The Galerkin finite element approach is particularly simple and widely used in practice [6].

2.2. Truncation error control and adaptive time step selection

The adaptive time stepping algorithm is presented for the pressure form of Richards equation and later extended to the mixed form. When applied to the spatially discrete pressure form

$$\mathbf{C}\frac{\mathrm{d}\boldsymbol{\psi}}{\mathrm{d}t}+\mathbf{K}\boldsymbol{\psi}=\mathbf{F}, \tag{8}$$

the backward Euler scheme, an $\mathrm{O}(\Delta t)$ approximation to (8), can be written as

$$\left[\mathbf{C}^{n+1}+\Delta t\mathbf{K}^{n+1}\right]\dot{\boldsymbol{\psi}}^{n+1}=-\mathbf{K}^{n+1}\boldsymbol{\psi}^{n}+\mathbf{F}^{n+1}, \tag{9}$$

$$\boldsymbol{\psi}_{(1)}^{n+1}=\boldsymbol{\psi}^{n}+\Delta t\dot{\boldsymbol{\psi}}^{n+1}, \tag{10}$$

where $\mathbf{C}$ is the mass matrix. For 1D flows and linear elements, a lumped elemental mass matrix is given by

$$\mathbf{C}^{(e)}=\frac{L^{(e)}}{2}\begin{bmatrix}(\mathrm{d}\theta/\mathrm{d}\psi+S_\mathrm{s}\theta/\phi)_1&0\\0&(\mathrm{d}\theta/\mathrm{d}\psi+S_\mathrm{s}\theta/\phi)_2\end{bmatrix}. \tag{11}$$

The accuracy of the approximation can be raised to $\mathrm{O}(\Delta t^2)$ by averaging the derivative estimates:

$$\boldsymbol{\psi}_{(2)}^{n+1}=\boldsymbol{\psi}^{n}+\frac{1}{2}\Delta t(\dot{\boldsymbol{\psi}}^{n}+\dot{\boldsymbol{\psi}}^{n+1}). \tag{12}$$

A measure of the absolute local truncation error of the backward Euler approximation (10) is given by the difference between (10) and (12):

$$\mathbf{e}^{n+1}=\frac{1}{2}\Delta t\left|\dot{\boldsymbol{\psi}}^{n}-\dot{\boldsymbol{\psi}}^{n+1}\right|. \tag{13}$$

Eq. (12) can be shown to correspond to a member of the Thomas–Gladwell integration family [19] with the weighting parameters selected to make the Thomas–Gladwell non-linear system identical to (9) and enforce $\mathrm{O}(\Delta t^2)$ accuracy [8]. Approximations (10) and (12) are

both unconditionally stable [18,19,22], and thus well suited for stiff ODE systems such as the spatially discrete Richards equation.

An error test takes place following the estimation of the local truncation error. In order to generalise the approach to simulations of flows in both saturated and unsaturated media (where pressure ψ may approach zero), a mixed absolute-relative error test is employed. The time step is accepted if the following condition is satisfied.

$$\max_i(e_i^{n+1} - \tau_R \mid \psi_i^{n+1} \mid -\tau_A) < 0, \tag{14}$$

where τ_A and τ_R are, respectively, an absolute and relative truncation error tolerance and i indexes the nodes in the spatial mesh. The node index with the largest mixed measure of the error is stored as iCrit to be used in the stepsize selectors described below. The mixed type of error control is robust and works for all ranges of the solution [5]. It can be observed that as $|\psi| \to 0$, the test becomes dominated by the absolute error criterion, while if $|\psi|$ is large, the procedure is governed by the relative error restriction. If a strictly relative error test is necessary, τ_A can be set to 0, while setting $\tau_R = 0$ leads to the standard absolute error test.

If the current time step is accepted, the stepsize for the next time step is calculated using

$$\Delta t_1^{n+1} = \Delta t^n \times \min\left(s\sqrt{\frac{\tau_R\left|\psi_{i\mathrm{Crit}}^n\right| + \tau_A}{\max(e_{i\mathrm{Crit}}^n, EPS)}}, r_{\max}\right). \tag{15}$$

Conversely, if the time step is rejected, it is re-attempted with a reduced stepsize based on the latest error estimate

$$\Delta t_{j+1}^{n+1} = \Delta t_j^{n+1} \times \max\left(s\sqrt{\frac{\tau_R \mid \psi_{i\mathrm{Crit},j}^{n+1} \mid +\tau_A}{\max(e_{i\mathrm{Crit},j}^{n+1}, EPS)}}, r_{\min}\right), \tag{16}$$

where j indexes the recursive stepsize reduction. The multiplier constraints $r_{\min} \cong 0.1$ and $r_{\max} \cong 4.0$, the safety factor $s \cong 0.8$–0.9 and the machine constant EPS ($\sim 10^{-10}$) are incorporated to increase the robustness of the algorithm by guarding against spuriously large or small stepsize changes, as well as against time steps that just fail to meet the error tolerance. These precautions are necessary because the truncation error measure (13) is not exact and may contain numerical noise.

The chief advantage of the method is that it leads to a consistent and efficient variation of stepsize, supplies accurate initial estimates for the non-linear iteration and provides insights into the suitability of the spatial discretisation. The scheme performs excellently in elasto-plastic consolidation simulations [17] and is also highly effective for the solution of the moisture form of Richards equation [8]. The extension of the approach to the more general mixed form of Richards equation hinges on adequate treatment of both state variables, moisture and pressure, in the temporal approximation.

2.3. The modified Picard (chord slope) approximation

The classic method of Celia et al. [3] is based on a backward difference approximation to $\mathrm{d}\boldsymbol{\theta}/\mathrm{d}t$ in (4):

$$\mathbf{M}^{n+1}\frac{\boldsymbol{\theta}^{n+1} - \boldsymbol{\theta}^n}{\Delta t} + \mathbf{K}^{n+1}\boldsymbol{\psi}^{n+1} + \mathbf{F}^{n+1} = 0, \tag{17}$$

This non-linear system can be solved using a modified fixed-point (modified Picard) iteration:

$$\begin{aligned}[\mathbf{C}^{n+1,m} + \Delta t\mathbf{K}^{n+1,m}]\delta\boldsymbol{\psi}^{m+1} \\ = -\{\Delta t(\mathbf{F}^{n+1,m} + \mathbf{K}^{n+1,m}\boldsymbol{\psi}^{n+1,m}) \\ + \mathbf{M}^{n+1,m}(\boldsymbol{\theta}^{n+1,m} - \boldsymbol{\theta}^n)\},\end{aligned} \tag{18}$$

$$\boldsymbol{\psi}^{n+1,m+1} = \boldsymbol{\psi}^{n+1,m} + \delta\boldsymbol{\psi}^{m+1}. \tag{19}$$

Eqs. (18) and (19) will be referred to as the Celia et al. solution to Richards equation. In the Celia et al. scheme, $\mathrm{d}\theta/\mathrm{d}\psi$ in the $\mathbf{C}$ matrix (11) is evaluated analytically. Rathfelder and Abriola [15] showed that the Celia et al. scheme is equivalent to a pressure-based backward Euler formulation (9), with the specific capacity $\mathrm{d}\theta/\mathrm{d}\psi$ approximated using a chord-slope estimate:

$$\left(\frac{\mathrm{d}\theta}{\mathrm{d}\psi}\right)^{n+1} \cong \frac{\Delta\theta}{\Delta\psi} = \frac{\theta^{n+1} - \theta^n}{\psi^{n+1} - \psi^n}. \tag{20}$$

A Taylor series analysis shows the truncation error of the approximation (20) to be

$$\begin{aligned}\varepsilon_{\mathrm{CS}}^{n+1} &= \frac{\psi^{n+1} - \psi^n}{2}\left(\frac{\mathrm{d}^2\theta}{\mathrm{d}\psi^2}\right)^{n+1} + \mathrm{O}(\Delta\psi^2) \\ &= \frac{\Delta t}{2}\left(\frac{\mathrm{d}\psi}{\mathrm{d}t}\frac{\mathrm{d}^2\theta}{\mathrm{d}\psi^2}\right)^{n+1} + \mathrm{O}(\Delta t^2)\end{aligned} \tag{21}$$

and hence the chord-slope approximation is $\mathrm{O}(\Delta t)$, i.e., first-order accurate in time. Since the Celia et al. scheme and its chord-slope equivalent approximate the mass matrix $\mathbf{C}^{n+1}$ in (8) using (20), they incur additional $\mathrm{O}(\Delta t)$ error and can not form the basis for $\mathrm{O}(\Delta t^2)$ algorithms.

2.4. A new second-order approximation to the mixed form of Richards equation

In order to obtain a mass conservative and pressure-based formulation that is $\mathrm{O}(\Delta t^2)$, the following quadratic approximation to the moisture time derivative at t^{n+1} can be applied to (4).

$$\left(\frac{\mathrm{d}\boldsymbol{\theta}}{\mathrm{d}t}\right)^{n+1} \cong \dot{\boldsymbol{\theta}}^{n+1} = \frac{2(\boldsymbol{\theta}^{n+1} - \boldsymbol{\theta}^n) - \Delta t\dot{\boldsymbol{\theta}}^n}{\Delta t} + \mathrm{O}(\Delta t^2). \tag{22}$$

The form of (22) closely resembles the derivative approximations implicitly used by other $\mathrm{O}(\Delta t^2)$ formulations, including the Thomas–Gladwell family. It avoids

multi-level constructs and their awkward implementation in variable-stepsize algorithms.

Substitution of the approximation (22) into the semi-discrete system (4) leads to a non-linear algebraic system implicity approximating Richards equation at the $(n+1)$th time level.

$$\mathbf{M}\left[\frac{2(\boldsymbol{\theta}^{n+1}-\boldsymbol{\theta}^{n})-\Delta t\dot{\boldsymbol{\theta}}^{n}}{\Delta t}\right]+\mathbf{K}^{n+1}\boldsymbol{\psi}^{n+1}=\mathbf{F}^{n+1}. \tag{23}$$

Functional (fixed-point) iteration with iteration counter m is used to linearise the system

$$\mathbf{M}\left[\frac{2(\boldsymbol{\theta}^{n+1,m+1}-\boldsymbol{\theta}^{n})-\Delta t\dot{\boldsymbol{\theta}}^{n}}{\Delta t}\right]+\mathbf{K}^{n+1,m}\boldsymbol{\psi}^{n+1,m+1}=\mathbf{F}^{n+1,m}. \tag{24}$$

A quasi-Newton approach, similar to that of Celia et al. [3], is employed to reduce the system to a single unknown vector. At a typical node i, the following expansion is used

$$\theta_i^{n+1,m+1}=\theta_i^{n+1,m}+\left(\frac{\mathrm{d}\theta}{\mathrm{d}\psi}\right)_i^{n+1,m}(\psi_i^{n+1,m+1}-\psi_i^{n+1,m})+\mathrm{O}(\delta\psi_i^2), \tag{25}$$

where $\delta\psi_i^{m+1}=\psi_i^{n+1,m+1}-\psi_i^{n+1,m}$. Inserting the Taylor expansion (25) into the linearised system (24) and rearranging yields the following linear system

$$[2\mathbf{C}^{n+1,m}+\Delta t\mathbf{K}^{n+1,m}]\delta\boldsymbol{\psi}^{m+1}=\{\mathbf{M}(2(\boldsymbol{\theta}^{n+1,m}-\boldsymbol{\theta}^{n})+\Delta t\dot{\boldsymbol{\theta}}^{n})+\Delta t(\mathbf{F}^{n+1,m}-\mathbf{K}^{n+1,m}\boldsymbol{\psi}^{n+1,m})\}, \tag{26}$$

$$\boldsymbol{\psi}^{n+1,m+1}=\boldsymbol{\psi}^{n+1,m}+\delta\boldsymbol{\psi}^{m+1}, \tag{27}$$

where $\mathbf{C}^{n+1,m}$, the non-linear capacitance matrix (11), is evaluated analytically. After each iteration, all variables are updated using $\boldsymbol{\psi}^{n+1,m+1}$ as the argument. Iterations proceed until

$$\max_i(|\delta\psi_i^{n+1,m+1}|-\tau_{PI(\mathrm{R})}\,|\psi_i^{n+1,m+1}|-\tau_{PI(\mathrm{A})})<0, \tag{28}$$

where $\tau_{PI(\mathrm{A})}$ and $\tau_{PI(\mathrm{R})}$ are, respectively, an absolute and relative iteration convergence tolerance. The mixed absolute-relative nature of the iteration convergence test (28) is consistent with the mixed absolute-relative truncation error test (14) in the time integrator.

Nørsett and Thomsen [12] have shown that, in general, it is not necessary to set $\tau_{PI}<\tau$. However, in a practical implementation, it may be prudent to do so to ensure that residual non-linear solver errors do not exceed the local temporal truncation error in unfavourable circumstances.

The vector $\dot{\boldsymbol{\theta}}^{n+1}$, required for the following time step as $\dot{\boldsymbol{\theta}}^{n}$, is then back-computed using (22).

The poor mass balance in many pressure-based approximations of Richards equation arises due to the presence of the analytic moisture capacity function $\mathrm{d}\theta/\mathrm{d}\psi$ [15]. It can be seen from (25) and (26) that, as the iterations converge and $\delta\psi\to 0$, the influence of $\mathrm{d}\theta/\mathrm{d}\psi$ on the numerical solution vanishes. In fact, mass balance errors vanish quadratically with τ_{PI} and can be made arbitrarily small by a sufficiently stringent iteration tolerance.

2.5. Truncation error control for the new second-order scheme

Internal consistency monitoring and adaptive time step variation are now developed. Moisture derivatives are unsuitable for the evaluation of the trunction error, since they vanish at saturated nodes. Instead, it is better to use to a posteriori estimates of the pressure derivatives $\dot{\boldsymbol{\psi}}$. Adaptive ODE solvers often control the stepsize selection according to estimates of the local truncation error of a lower-order approximation. This improves the reliability of the numerical integrator and makes the actual errors linearly related to the user tolerance [16]. Since (23) is $\mathrm{O}(\Delta t^2)$ accurate, the error measure (13) derived by Sloan and Abbo [17] and Kavetski et al. [8] for the $\mathrm{O}(\Delta t)$ backward Euler scheme is a suitable choice. The pressure derivatives for Eq. (13) are then given by backward differences

$$\dot{\boldsymbol{\psi}}^{n+1}=\frac{\boldsymbol{\psi}^{n+1}-\boldsymbol{\psi}^{n}}{\Delta t^{n+1}}+\mathrm{O}(\Delta t). \tag{29}$$

The adaptive time approximation then proceeds by testing the relative error estimate using condition (14) and selecting the appropriate stepsize according to Eqs. (15) or (16).

2.6. Initialisation of the adaptive time stepping scheme

Both $\dot{\boldsymbol{\theta}}(t=0)$ and $\dot{\boldsymbol{\psi}}(t=0)$ must be obtained prior to the first time step. The initial pressure derivative $\dot{\boldsymbol{\psi}}^0$ can be obtained by inverting the pressure-based ODEs (8):

$$\dot{\boldsymbol{\psi}}^0=[\mathbf{C}^0]^{-1}\{-\mathbf{K}^0\boldsymbol{\psi}^0+\mathbf{F}^0\}. \tag{30}$$

The initial moisture derivative $\dot{\boldsymbol{\theta}}^0$ can then be evaluated via the analytical chain rule:

$$\dot{\theta}_i^0=\left(\frac{\mathrm{d}\theta}{\mathrm{d}\psi}\right)_i^0\dot{\psi}_i^0. \tag{31}$$

The evaluation of the derivatives via (30) and (31) is exact and therefore does not degrade the order of accuracy or the mass balance of the approximation (23).

Note that, in general, at the $(n+1)$th time step, the derivatives $\dot{\boldsymbol{\theta}}^n$ and $\dot{\boldsymbol{\psi}}^n$ are re-used from the previous, nth time step and hence (30) and (31) are used at the first time step only. If explicit evaluation of the derivatives $\dot{\boldsymbol{\theta}}^n$ and $\dot{\boldsymbol{\psi}}^n$ is performed at each time step, then the scheme is similar to an implicit Runge–Kutta scheme that is only conditionally stable. The conditional stability of the first

time step is not problematic for two reasons: (i) only a single time step with (30) and (31) is performed, preventing the growth of potential instabilities and (ii) if the error in the tentative first step is too large, the error controller will reduce the stepsize until the error tolerance is met.

A consistent estimate of the first time step Δt_0 completes the algorithm:

$$\Delta t_0 = \min\left[(t_{\text{output}} - t_0), \min_i\left(s\frac{\sqrt{\tau_R}\,|\psi_i^0| + \sqrt{\tau_A}}{\max(|\dot{\psi}_i^0|, EPS)}\right)\right]. \tag{32}$$

This procedure (described by Shampine [16]) provides a reliable approach to Δt_0-selection, taking into account the distance to the first output point t_{output}, the expected solution behaviour given by $\dot{\boldsymbol{\psi}}_0$ and the mixed absolute-relative character of the error control.

2.7. Intermediate output times

An efficient treatment of output times can be accomplished by the "look-ahead" technique:

1. Check whether t_{output} can be reached in a single step Δt^{n+1}, i.e., $t_{\text{current}} + \Delta t^{n+1} \geqslant t_{\text{output}}$;
2. Yes $\Rightarrow$ truncate Δt to produce output at t_{output} : $\Delta t^{n+1} = t_{\text{output}} - t_{\text{current}}$. Perform time step;
3. No $\Rightarrow$ check whether t_{output} can be reached in two steps Δt^{n+1}, i.e., $t_{\text{current}} + 2\Delta t^{n+1} \geqslant t_{\text{output}}$;
4. Yes $\Rightarrow$ equalise the time steps, that, is set $\Delta t^{n+1} = 1/2(t_{\text{output}} - t_{\text{current}})$. Perform time step;
5. No $\Rightarrow$ proceed with un-altered time step Δt^{n+1}.

The chief advantage of this approach is that it avoids undesirable abrupt changes in time step size [16].

2.8. Non-linear iteration: accurate initial estimates

In order to provide accurate initial estimates for the iterative process and accelerate its convergence, linear or quadratic extrapolation can be undertaken. The quadratic estimate is given by

$$\boldsymbol{\psi}^{n+1,0} = \boldsymbol{\psi}^n + \Delta t^{n+1}\dot{\boldsymbol{\psi}}^n + \frac{1}{2}(\Delta t^{n+1})^2\ddot{\boldsymbol{\psi}}^{n-1}. \tag{33}$$

The acceleration $\ddot{\boldsymbol{\psi}}^n$ is given by the finite difference $\ddot{\boldsymbol{\psi}}^{n-1} = (\dot{\boldsymbol{\psi}}^n - \dot{\boldsymbol{\psi}}^{n-1})/\Delta t^n$. The estimate (33) is clearly more consistent with the $O(\Delta t^2)$ accuracy of the governing approximation than the commonly used $\boldsymbol{\psi}^{n+1,0} = \boldsymbol{\psi}^n$. The reliability of (33) is enhanced by the truncation error controller, which enforces solution linearity within the time step, that is, $1/2(\Delta t^{n+1})^2\ddot{\psi}_i^n/\psi_i^{n+1} \propto \tau_R \ll 1$ for all nodes. Since $\ddot{\boldsymbol{\psi}}^{n-1} \approx \ddot{\boldsymbol{\psi}}^n + O(\Delta t)$, the truncation error of the prediction (33) is also reduced, improving the accuracy of the extrapolation.

2.9. The discrete chain rule

The lack of mass conservation in standard pressure-based numerical models of Richards equation has been attributed to a failure to satisfy a discrete equivalent of the chain rule [15]. The chord-slope pressure-based scheme of Rathfelder and Abriola [15] employs a first-order approximation to the analytic chain rule to enforce correct mass balance:

$$\frac{\partial\theta}{\partial t} = \left\{\frac{\mathrm{d}\theta}{\mathrm{d}\psi}\right\}\frac{\partial\psi}{\partial t}$$
$$\Rightarrow \frac{\theta^{n+1} - \theta^n}{\Delta t} = \left\{\frac{\theta^{n+1} - \theta^n}{\psi^{n+1} - \psi^n}\right\}\frac{\psi^{n+1} - \psi^n}{\Delta t} + O(\Delta t). \tag{34}$$

The new scheme (23) can also be derived from the pressure-based ODEs if a higher-order discrete form of the chain rule is employed to approximate the specific capacity $\mathrm{d}\theta/\mathrm{d}\psi$.

$$\frac{\partial\theta}{\partial t} = \left\{\frac{\mathrm{d}\theta}{\mathrm{d}\psi}\right\}\frac{\partial\psi}{\partial t}$$
$$\Rightarrow \frac{2(\theta^{n+1} - \theta^n) - \Delta t\dot{\theta}^n}{\Delta t}$$
$$= \left\{\frac{2(\theta^{n+1} - \theta^n) - \Delta t\dot{\theta}^n}{2(\psi^{n+1} - \psi^n) - \Delta t\dot{\psi}^n}\right\} \times \frac{2(\psi^{n+1} - \psi^n) - \Delta t\dot{\psi}^n}{\Delta t} + O(\Delta t^2). \tag{35}$$

The specific capacity is hence approximated by the ratio of the time rates of its components. This observation theoretically justifies the mass conservative properties of (26), established empirically under both uniform and variable-stepsize conditions.

3. Results and discussion

An empirical assessment of the proposed time stepping scheme is carried out by solving the vertical infiltration problem analysed by Celia et al. [3] and Rathfelder and Abriola [15]. The 60-cm column of New Mexico soil is parameterised by the following van Genuchten relationships:

$$\theta(\psi) = \frac{\theta_s - \theta_r}{[1 + (\alpha\,|\,\psi\,|)^n]^m} + \theta_r, \tag{36}$$

$$K(\psi) = K_s\frac{\left\{1 - (\alpha\,|\,\psi\,|)^{n-1}[1 + (\alpha\,|\,\psi\,|)^n]^{-m}\right\}^2}{[1 + (\alpha\,|\,\psi\,|)^n]^{m/2}}, \tag{37}$$

where the saturated hydraulic conductivity $K_s = 0.00922$ cm/s, residual moisture content $\theta_r = 0.102$, saturated moisture content $\theta_s = 0.368$ and the parameters are given as $\alpha = 0.0335$, $n = 2$, $m = 0.5$. Boundary conditions are chosen as $\psi(z = 0,\ t) = -75$ cm and

$\psi(z = 60,\ t) = -1000$ cm. The initial pressure profile is specified as

$$\psi(z, t = 0) = \begin{cases} -1000, & z \geqslant 0.6, \\ -75 - \frac{925}{0.6} z, & 0 \leqslant z < 0.6. \end{cases} \quad (38)$$

These forcing conditions lead to the development of a sharp infiltration front and induce large gradients in the solution. This type of problem provides a rigorous test case for time integrators and is well suited for the analysis of numerical convergence and efficiency.

We also note that nothing in the time stepping algorithm precludes its use for 2D and 3D spatial configurations. The only difference is the structure of the finite element (or finite difference) matrices **M**, **K** and **F**. An analysis of the influence of these changes is important, but separate to the time integration per se; it could be an area for further research.

In order to simplify the evaluation of the scheme, the absolute temporal error tolerance τ_A and the absolute iteration error tolerance $\tau_{PI(A)}$ are set to zero, thus enforcing a strict relative error test. In the remainder of the text, τ refers to τ_R and τ_{PI} refers to $\tau_{PI(R)}$.

A surrogate "exact" solution is evaluated numerically by the adaptive scheme with a truncation error tolerance $\tau = 10^{-7}$ and an iteration tolerance $\tau_{PI} = 10^{-9}$. Unless stated otherwise, a uniform finite element mesh with 100 linear elements is used. It is noted that the mesh type and configuration affect spatial errors. When temporal errors alone are assessed, spatial errors can conveniently be excluded by employing identical spatial approximations. The difference between the trial and exact solutions of the ODEs is then pure time discretisation error, which is to be controlled by the proposed algorithm.

The propagation of the solution through the domain is shown in Fig. 1. Results of the adaptive scheme with $\tau = 10^{-2}$ are already indistinguishable from the exact solution at any time within the simulation. Fig. 1 shows the formation of a steep infiltration front (shock) and its wave-like propagation through the soil column. Temporal (and spatial) gradients within the highly non-linear region at the toe of the shock vary significantly.

The ability of the adaptive scheme to control temporal errors is assessed using an error measure defined as

$$\varepsilon(t^n, \tau) = \max_i \left| \frac{\psi_i^n - \bar{\psi}_i^n}{\bar{\psi}_i^n} \right|, \quad (39)$$

where $\bar{\psi}_i^n$ is the exact solution and i indexes the nodes in the spatial mesh. The evolution of the error is shown in Fig. 2 and is obtained by computing the exact and approximate solutions at a series of a priori specified output times. As Fig. 2 shows, the adaptive integration constrains the global errors throughout the simulation within the prescribed limits, with the actual errors being linearly related to the tolerance. In fact, $\varepsilon(t, \tau) \sim 0.1\tau$. The second-order convergence of the adaptive scheme is evident from Table 1 (which presents the statistics of the runs shown in Fig. 2), with the number of successful time steps decreasing by a factor of $\approx\sqrt{10}$ for a reduction in error by a factor of $\approx$10. The number of steps where the scheme failed to meet the error tolerance (and it was necessary to re-attempt the time step with a smaller stepsize) is small in all cases, below 1% of the number of successful steps.

The performance of the new automatic time stepping algorithm can be compared with results of the Celia et al. scheme, shown in Table 2. The Celia et al. scheme is coupled with a heuristic time step selector described by Rathfelder and Abriola [15]. When the number of Picard iterations falls below N_{inc}, the stepsize for the next time step is increased by a factor of $F_{inc}(> 1)$. When the number of iterations exceeds N_{dec}, the next time step is multiplied by $F_{dec}(< 1)$. Table 2 shows that error is

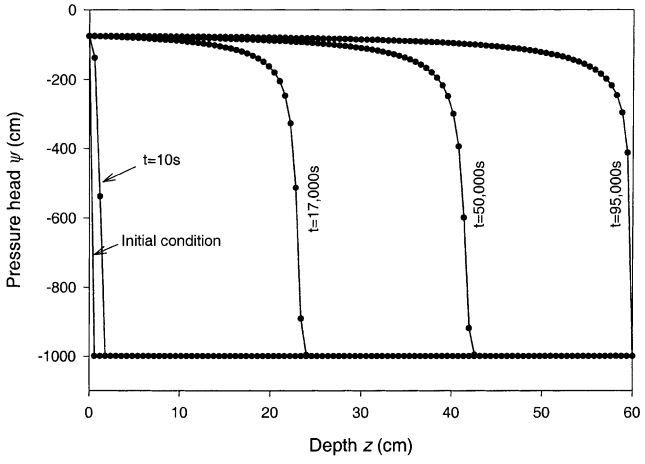

Fig. 1. Solution of the test problem: pressure profiles at various times throughout the simulation. The approximate solution was obtained using the adaptive scheme with $\tau = 0.01$ and $\tau_{PI} = 10^{-4}$.

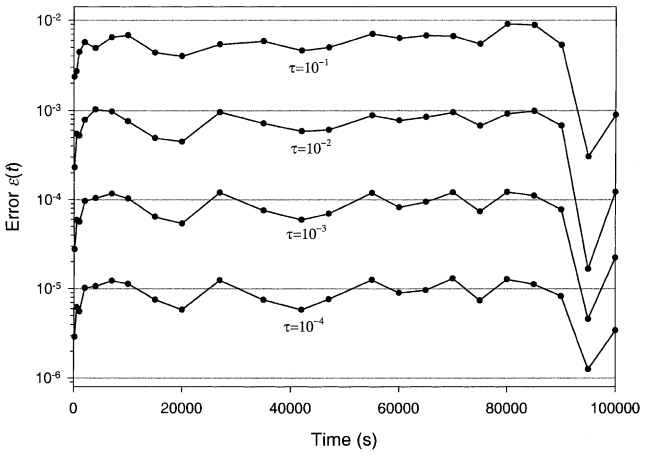

Fig. 2. Relation between the user-prescribed temporal error tolerance τ and the actual temporal errors $\epsilon(t)$ for the adaptive scheme.

Table 1
Performance statistics for the automatic scheme[a]

Error tolerance τ, ($\tau_{Pf} = 0.01\tau$)	Maximum error max(ε)	Number of successful steps	Number of failed steps	Number of iterations	CPU time (s)
10^{-1}	9.1×10^{-3}	256	2	1053	1.4
10^{-2}	1.0×10^{-3}	731	1	2230	3.1
10^{-3}	1.2×10^{-4}	2242	1	6557	9.0
10^{-4}	1.3×10^{-5}	6988	1	16,818	23

[a] CPU times refer to runs on a Pentium II 350 MHz processor with 128 MB SDRAM. 32-bit precision used in all calculations.

Table 2
Results of empirical optimisation of the Celia et al. algorithm with the heuristic time step selection to produce uniform temporal error profiles[a]

Iteration tolerance τ_{Pf}	N_{inc}/F_{inc}	N_{dec}/F_{dec}	Maximum error max(ε)	Number of time steps	Number of iterations	CPU time (s)
10^{-2}	3/1.05	15/0.9	1.53×10^{-1}	382	843	1.2
10^{-4}	2/1.02	3/0.9	1.05×10^{-2}	4697	9016	12
10^{-5}	2/1.01	3/0.9	3.28×10^{-3}	14,944	28,506	39

[a] $\Delta t_0 = 0.1$ s. Note that the CPU times (PII 350) listed do not include the time spent manually optimising the heuristic parameters.

linearly related to the number of time steps, indicating that the scheme is first-order accurate in time.

In this study, the computational efficiency of the schemes is compared on the basis of the total number of iterations required by the algorithm to achieve a certain error. It is noted that the overhead cost of the automatic time step selection is very small compared with the cost of matrix formation and inversion at each non-linear iteration. The slower convergence of the Celia et al. solution with heuristic stepsize selection makes the scheme inefficient when errors of 1.0–0.1% and below are required. For example, 4697 time steps (9016 iterations) are required for the Celia et al. scheme to yield an accuracy of 10^{-2} (1%). The new adaptive algorithm requires only 256 time steps (1053 iterations) for the same accuracy. CPU times reflect these observations, with the adaptive scheme using ~1.4 s and the heuristic scheme 12 s on PII 350 MHz machine. These are worthwhile savings in computational effort, especially when considering benefits for larger problems. The relative efficiency of the second-order adaptive scheme increases further as finer accuracy requirements are imposed. It is also noted that the improved initial estimate (33) for the non-linear solver in the Celia et al. scheme has been used. More iterations would have been required if the standard approach ($\boldsymbol{\psi}^{n+1,0} = \boldsymbol{\psi}^n$) was used.

In comparison, the use of uniform time steps (not shown here) leads to large, of the order of 100%, errors in the initial flows and is thus inappropriate.

It is of practical interest to examine the pattern of stepsize variation, shown in Fig. 3. The stepsize evolution revealed in Fig. 3 is generally intuitive. Early times are characterised by rapid and non-linear moisture flows due to abrupt forcing, while during the remainder of the simulation, as the infiltration front attains its terminal velocity and shape, an increase in stepsize is appropriate.

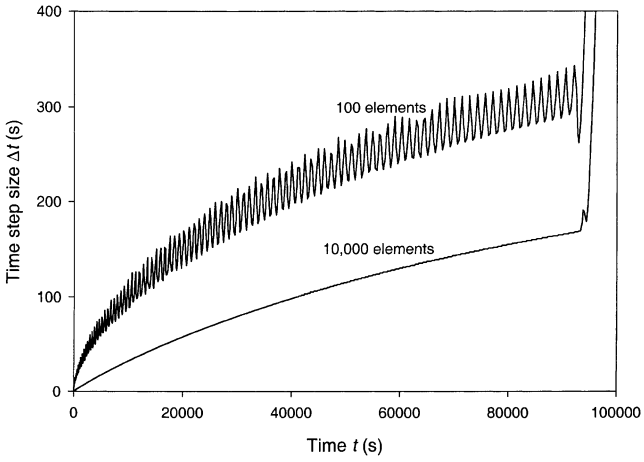

Fig. 3. Time step variation throughout the integration with 100 and 10,000 spatial elements.

The automatic algorithm is also able to detect the steady state condition once the infiltrating front reaches the boundary of the solution domain (at $t \sim 95{,}000$ s) and increases the time step accordingly.

The number of iterations at each step of the adaptive scheme is fairly constant, 3–4 iterations per step for the 100-element simulation and 4 iterations per step for the 10,000-element solution. This suggests that the heuristic guidelines for stepsize adjustment based on constraining the time step to maintain a constant number of iterations per step are qualitatively valid. However, the optimal values of the heuristic settings may vary throughout the integration. Since the heuristic technique is normally implemented with fixed time step acceleration parameters for the entire integration, it cannot operate as efficiently as the new algorithm, which continuously varies the stepsize multipliers to meet the requested error tolerance.

The technique used to regulate the stepsize is important for both accuracy and efficiency, and the theoretically based approach presented in this paper clearly provides more control over the temporal approximation error. Its central appeal is the fully automatic stepsize selection, simplifying the task of the user and also reducing the ultimate CPU cost of the solution of a given problem.

A major disadvantage of the heuristic algorithm is its requirement for manual optimisation in a series of runs with trial parameters. This procedure relies heavily on the ability and experience of the user. Conversely, the automatic algorithm requires a single run to automatically optimise the stepsize selection and perform the integration. In a practical situation, a verification of the results by using a series of tolerances (e.g., $10^{-2} \rightarrow 10^{-3} \rightarrow 10^{-4}$) is recommended to ensure that consistent results are being obtained. Such verification procedure must be performed after any numerical solution, be it a simple scheme or a sophisticated black-box integrator. The advantage of the proposed adaptive scheme over fixed or heuristic time steppers is that each new run with a different tolerance will be automatically optimised by the error control mechanism. Conversely, the user of a heuristic scheme must carry out both (i) optimisation for efficiency and (ii) verification of accuracy.

The sensitivity of the adaptive scheme to the safety factor s in (15) and (16) is shown in Fig. 4. The figure shows the trade-off between a more conservative approach to time stepping (smaller s), resulting in more time steps but less iterations (since the non-linearities are lesser and more amenable to iterative solution), and a more aggressive approach (larger s), leading to less steps but more iterations. The number of failed steps is small unless s is very close to 1. The optimum s, corresponding to the minimum number of iterations (including both successful and failed steps), is 0.8. Other values of s do not lead to excessive losses of efficiency, attesting to the operational robustness of the algorithm. The bounds $r_{\min} = 4.0$ and $r_{\max} = 0.1$ have negligible impact on the simulation, confirming that no drastic time step changes were necessary. Conversely, the performance of the heuristic scheme is quite sensitive to all four heuristic parameters (and the iteration tolerance), further complicating its optimisation and verification.

Having demonstrated the utility of the adaptive scheme for accurate and efficient handling of the time dependence of variably saturated flows, it is of interest to examine its compatibility with the spatial discretisation. Indeed, the oscillations in stepsize (Fig. 3), which appear associated with abrupt interelemental transition of the moisture front in the crude mesh, suggest that the time step history can be used for an indirect assessment of the adequacy of the spatial mesh. Fig. 5 shows the influence of the number of elements in the spatial grid on the number of time steps selected by the adaptive scheme with the tolerance τ of 1%. Also shown is the total number of iterations in the simulation and an average Courant number Cr_{avg}, calculated as

$$Cr = v\frac{\Delta t}{\Delta z} \approx Cr_{\text{avg}} = v_{\text{avg}}\frac{\Delta t_{\text{avg}}}{\Delta z} = \frac{Lz}{Lt}\left(\frac{Lt}{Nt}\Big/\frac{Lz}{Nz}\right) = \frac{Nz}{Nt}, \tag{40}$$

where v is the velocity at which the solution front propagates through the spatial domain, Lz and Lt denote, respectively, the spatial and temporal dimensions of the domain and Nz and Nt are the number of elements in the spatial mesh and the number of time steps selected by the automatic scheme. The infiltration velocity is approximated as $v_{\text{avg}} = Lz/Lt$, since the duration of the simulation corresponds roughly to the front travelling across the entire depth. It is noted that, since the stepsize increases as the simulation proceeds (Fig. 3), the Courant number at the end of the simulation will be

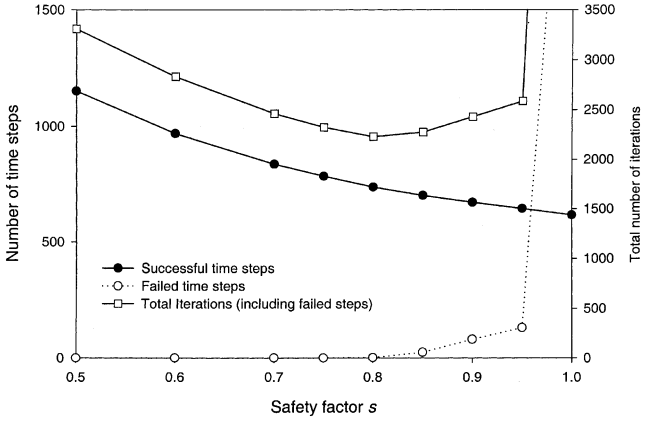

Fig. 4. Sensitivity of the adaptive scheme to the safety factor s. The following settings are used: $\tau = 0.01$, $\tau_{PI} = 10^{-4}$, $r_{\max} = 4$ and $r_{\min} = 0.1$. 100 spatial elements are employed.

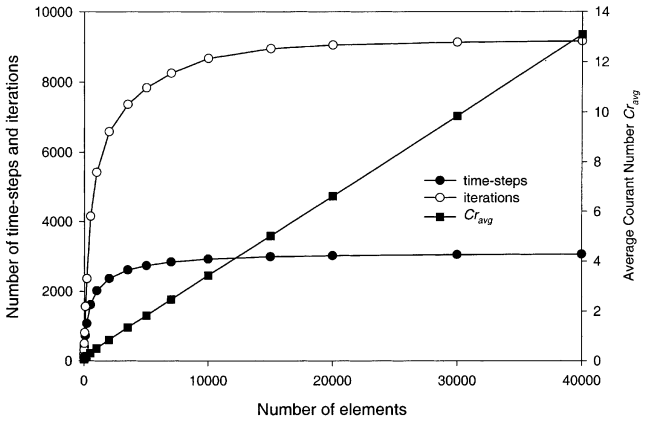

Fig. 5. Effect of the number of spatial elements on the performance of the adaptive time stepping scheme. The temporal truncation error tolerance is fixed at 1%.

substantially larger than Cr averaged over the entire simulation period.

Fig. 5 shows that there is an asymptotic influence of the number of spatial elements in the mesh on the number of time steps taken by the adaptive scheme to obtain a certain temporal accuracy. Initially, as the spatial grid is refined, more time steps are required to achieve the same temporal accuracy. However, once a certain spatial accuracy is attained, further spatial refinement does not influence the behaviour of the adaptive temporal discretisation. When five elements are used, the average time step is 1055 s, while in the simulation with 40,000 elements the average time step is reduced to 33 s. The total number of iterations taken by the scheme also exhibits an asymptotic convergence pattern, reaching a plateau as the number of elements is increased beyond approximately 10,000. These results can be interpreted from the following point of view. As the number of elements in the grid increases, the ODE system (4) becomes effectively infinite and continuous in space, with negligible spatial discretisation errors. It is then intuitive that a further grid refinement will not change the behaviour of the ODE system and will not have an effect on the adaptive temporal integration.

The Courant number is often used as a stability criterion for explicit approximations to purely advective (hyperbolic) systems. Stability is ensured when

$$Cr = v\frac{\Delta t}{\Delta z} \leqslant 1. \tag{41}$$

The Courant criterion also applies to the stability of approximations to the family of advective–diffusive equations, including Richards equation [2]. In particular, Daus et al. [4] and Noorishad et al. [11] derive approximate Courant conditions for the formally stable Crank–Nicolson approximation to the standard advection–diffusion equation. Since Fig. 5 shows successful simulations where $Cr \gg 1$, it demonstrates that the Courant number is not a necessary condition for the stability of the adaptive time integration scheme, as expected for an unconditionally stable implicit scheme.

The value of the Courant number is that it provides a useful criterion for balancing the errors of the temporal and spatial approximations. Fig. 3 shows that the oscillations in the stepsize take place when the $Cr_{\text{avg}} < 1$ and are dramatically reduced when $Cr_{\text{avg}} > 1$. In the former case, the infiltrating wave shifts on average one element per time step, while the later condition corresponds to the infiltrating front traversing several elements in a single step. Time step oscillations are inconsistent with the smooth dissipative character of the solution. Hence, these oscillations suggest that the spatial grid should be refined to reduce the spatial errors and increase the smoothness of the ODE systems (4).

However, the approximation with 40,000 elements (Fig. 5) is evidently unbalanced: the dense spatial mesh provides no benefit since the overall accuracy is limited by the temporal errors. When using the adaptive time stepping scheme, a useful approach to balancing space–time accuracy is to specify an acceptable temporal error tolerance, and then refine the spatial grid until $Cr \sim 1$ and stepsize oscillations disappear. Further analysis is required to refine this heuristic rule as it may depend on the spatial approximation.

4. Conclusions

The study presents a new adaptive approximation technique for the numerical temporal integration of the mixed form of Richards equation. The algorithm is second-order accurate in time and is inherently mass conservative. Implementation of the adaptive error control leads to a consistent and efficient selection of time steps, constraining temporal errors below a user-prescribed error tolerance. An additional benefit of the algorithm is the availability of improved initial solution estimates for the initialisation of iterative non-linear solvers. Another feature of the adaptive time step selection is its interaction with the spatial approximation, with adequate spatial grids leading to a smooth time step size variation. It is shown that the adaptive time stepping procedure satisfies the primary objectives of accuracy and computational efficiency. The simplicity and effectiveness of the method make it an attractive approach for numerical simulations of variably saturated flows.

Further research could examine the performance of adaptive time stepping schemes in more complex flow cases, e.g., in 2D and 3D systems. Moreover, an important step forward would be to combine an adaptive time stepping scheme with an adaptive spatial grid generation procedure. This combined algorithm would control numerical errors comprehensively, rather than being limited to only the temporal discretisation. Indeed, an accurate approximation of a system with highly transient flow patterns requires a time-space grid that is dynamically adaptive in each dimension. Furthermore, the inter-relation between the temporal and spatial discretisation errors suggests that temporal and spatial grid adaptations will be mutually beneficial. Studies in these areas would address the current imbalance between the rigorous treatment of temporal errors and somewhat less-researched treatment of spatial errors in numerical approximations of Richards equation.

References

[1] Bergamaschi L, Putti M. Mixed finite elements and Newton-type linearizations for the solution of Richards' equation. Int J Numer Methods Engrg 1999;45:1025–46.

[2] Binning P, Celia MA. Practical implementation of the fractional flow approach to multi-phase flow simulation. Adv Water Resources 1999;22(5):86–95.

[3] Celia MA, Bouloutas ET, Zarba RL. A general mass-conservative numerical solution for the unsaturated flow equation. Water Resources Res 1990;26(7):1483–96.
[4] Daus AD, Frind EO, Sudicky EA. Comparative error analysis infinite element formulations of the advection–dispersion equation. Adv Water Resources 1985;8(June):86–95.
[5] Engeln-Mullges G, Uhlig F. Numerical algorithms with Fortran. Berlin: Springer; 1996.
[6] Huyakorn PS, Pinder GF. Computational methods in subsurface flow. San Diego: Academic Press; 1985.
[7] Ju SH, Kung KJS. Mass types, element orders and solution schemes for the Richards equation. Comput Geosci 1997; 23(2):175–87.
[8] Kavetski D, Binning P, Sloan SW. Adaptive backward Euler time stepping with truncation error control for numerical modelling of unsaturated fluid flow. Int J Numer Methods Engrg, submitted for publication.
[9] Lehmann F, Ackerer PH. Comparison of iterative methods for improved solutions of the fluid flow equation in partially saturated porous media. Transport in Porous Media 1998;31(3):275–92.
[10] Miller CT, Williams GA, Kelley CT, Tocci MD. Robust solution of Richards' equation for nonuniform porous media. Water Resources Res 1998;34(10):2599–610.
[11] Noorishad J, Tsang CF, Perrochet P, Musy A. A perspective on the numerical solution of convection dominated transport problems: a price to pay for the easy way out. Water Resources Res 1992;28(2):551–64.
[12] Norsett SP, Thomsen PG. Local error control in SDIRK-methods. BIT 1986;26:100–13.
[13] Paniconi C, Aldama AA, Wood EF. Numerical evaluation of iterative and noniterative methods for the solution of the nonlinear Richard's equation. Water Resources Res 1991; 27(6):1147–63.
[14] Press WH, Flannery BP, Teukolski SA, Vetterling WT. Numerical recipes: the art of scientific computing. New York: Cambridge University Press; 1986.
[15] Rathfelder K, Abriola LM. Mass conservative numerical solutions of the head-based Richards equation. Water Resources Res 1994;30(9):2579–86.
[16] Shampine LF. Numerical solution of ordinary differential equations. London: Chapman & Hall; 1994.
[17] Sloan SW, Abbo AJ. Biot consolidation analysis with automatictime stepping and error control. Part 1: theory and implementation. Int J Numer Anal Methods Geomech 1999;23:467–92.
[18] Smith GD. Numerical solution of partial differential equations: finite difference methods. Oxford: Clarendon Press; 1985.
[19] Thomas RM, Gladwell I. Variable-order variable-step algorithms for second-order systems. Part 1: the methods. Int J Numer Methods Engrg 1988;26:39–53.
[20] Tocci MD, Kelly CT, Miller CT. Accurate and economical solution of the pressure-head form of Richards' equation by the method of lines. Adv Water Resources 1997;20(1):1–14.
[21] Williams GA, Miller CT. An evaluation of temporally adaptive transformation approaches for solving Richards' equation. Adv Water Resources 1999;22(8):831–40.
[22] Wood WL. Practical time stepping schemes. Oxford: Oxford University Press; 1990.